

The ratio of active and reactive losses in drift step recovery diodes depending on their operating mode

© M.N. Cherenev^{1,2}, A.F. Kardo-Sysoev², A.G. Lyublinsky²

¹ St. Petersburg State Electrotechnical University „LETI“, St. Petersburg, Russia

² Ioffe Institute, St. Petersburg, Russia

E-mail: max50055@icloud.com

Received May 12, 2023

Revised July 14, 2023

Accepted October, 30, 2023

An experimental investigation and numerical modeling have been conducted to study the dependence between energy losses and the density of reverse current during the switching of a silicon $p^+ - p - n - n^+$ -structure (Drift Step Recovery Diode) from the conducting state to the blocking state. The active and reactive components of energy losses were separately calculated, and their ratio was analyzed depending on the switching parameters. It was shown that at low densities of reverse current, the structure can return up to 90% of the energy spent on recovering the voltage across the diode. As the density of reverse current increases, the proportion of active energy loss component increases.

Keywords: Drift Step Recovery Diode, nanosecond switch, opening diode switch, power semiconductors.

DOI: 10.61011/TPL.2023.12.57590.140A

High-voltage pulses of nanosecond and subnanosecond duration are used in ultra-wideband radar and communication systems [1]. The main requirements for generators for ultra-wideband systems are pulse amplitude from a few tens of volts to tens of kilovolts, repetition rates up to units of megahertz and higher, high efficiency, and low jitter. These requirements in combination with compact dimensions and long operation time can only be met by the use of semiconductor devices. The work considers open-circuit devices represented by drift step recovery diodes (DSRD) [2,3].

The physical principles of DSRD operation have already been developed [1,4], computer modelling of the processes of sharp current interruption has been carried out [5], many practical schemes of pulse generators based on them have been published [6,7], but the question of energy losses in DSRD during switching has been insufficiently covered. In [8] a quantitative evaluation of active energy losses during the charge extraction stage is given depending on the parameters of the duty cycle. In the present work, the ratios of active and reactive components of the energy losses in the process of current interruption in the diode are considered for the first time. The active component leads to diode heating, while the reactive component accumulates in the $p-n$ -junction capacitance and can return to the external circuit including the load. Information on the dependence of reactive losses on the operating mode of DSRD, their magnitude and ratio to the active component is important both for the development of circuit engineering solutions when building generators and for optimising the DSRD structure for a given operating mode.

Fig. 1 shows the circuit diagram of the bench for studying the parameters of the voltage pulse generated by DSRD.

A fast high-voltage n-channel MOSFET DE475-102N21A controlled by an IXYS IXRFD631 driver is selected as the primary switch M_1 . Voltage pulses are recorded with a Tektronix MSO64 digital oscilloscope with a bandwidth of 4 GHz. Aeroflex 18N10W coaxial attenuators with a bandwidth of 18 GHz are used as $50\ \Omega$ load equivalents and to attenuate the signal applied to the oscilloscope input. A low-inductance shunt R_{sh} with a nominal resistance of $1\ \Omega$ is used to record the current flowing through the DSRD. The voltage across the DSRD is equal to the voltage difference between U_{CH1} and U_{CH2} (thus eliminating the voltage drop across the shunt).

Initially capacitor C_2 is charged to the source voltage V_2 . When a voltage pulse of a given duration is applied from an external generator V_1 to the gate of the transistor M_1 , it turns-on, the capacitor C_2 discharges through the circuit inductance L_2 —DSRD—shunt and due to the direct current there is an injection of minority charge carriers into the base of the DSRD (diode pumping). The current is determined by the source voltage V_2 , the inductance L_1 , the capacitance C_2 and the duration of the reference pulse. At the moment of the end of the reference pulse transistor M_1 turns-off, the reverse current flows through the DSRD, providing the removal of minority charge carriers from the diode base. The reverse current is determined by the inductance L_2 , the transistor output capacitance M_1 , which is hundreds of picofarads, and the capacitance C_1 . At the moment of current interruption through the DSRD, the energy stored in the magnetic field of the inductance L_2 is thrown into the load R_{load} , forming a voltage pulse on it.

A series of experiments were carried out to determine the structure voltage (U), maximum switching speed

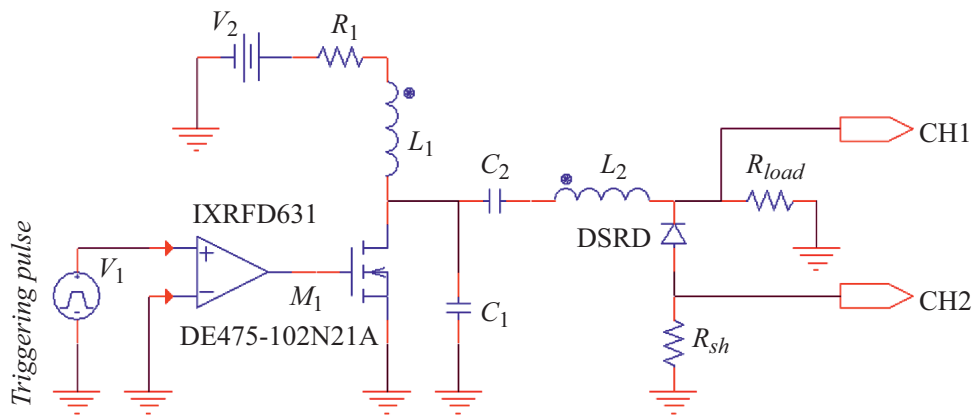


Figure 1. Circuit diagram of the measuring bench.

Characteristics of DSRD switching process at different reverse current densities

N ^o	S, mm ²	U, V	j, A/cm ²	dU/dt, V/ns	W _Σ , μJ/cm ²	W _r , μJ/cm ²	W _a , μJ/cm ²	W _r /W _Σ
1	4.5	570	372	671	86.9	47.6	39.3	0.55
1*	4.5	569	367	699	89.1	50.4	38.7	0.57
2	18	400	101	208	31	27.8	3.2	0.90
2*	18	420	101	192	33.9	28.8	5.1	0.85
3	18	559	140	292	55.3	44.5	10.8	0.80
3*	18	591	137	303	58.7	51.2	7.5	0.87

(dU/dt), energy loss (W_{Σ}), and separately the active (W_a), reactive (W_r) components and the ratio of reactive component to total energy loss (W_r/W_{Σ}). Epitaxial silicon $p^+-p-n-n^+$ structures of different area (S) designed for a reverse voltage of 500 V were used as DSRD. Experiments were performed at different reverse current densities (j) (see Table). Each experiment is matched to a computer simulation (numbers in the table are marked with an asterisk) performed in the TCAD Silvaco software package by jointly solving the Kirchhoff equations for the external equivalent electrical circuit and a one-dimensional diffusion-drift physical model of the electron-hole plasma dynamics in a DSRD-structure. A fundamental system of equations consisting of continuity equations, diffusion-drift transport equations, and Poisson's equation was used to calculate the plasma dynamics processes. When calculating the mobility of electrons and holes, its dependence on the electric field, scattering on lattice vibrations, electron-hole scattering and scattering on ionised impurities were taken into account. The standard model proposed in [9] was used to account for the saturation effect of carrier velocity in strong fields and, consequently, the reduction of electron and hole mobility. This model provides a smooth transition from weak fields to strong fields. The mobility in weak fields was calculated using the [10] model, which is preferable at high concentration of injected carriers typical for power semiconductor devices. To calculate the recombination

of electrons and holes, a simplified Shockley–Reed–Hall model was taken, the use of which is acceptable at high injection levels characteristic of power semiconductor devices. The dependence of the carrier lifetime on the impurity concentration [11–13] was also taken into account in the model. The difference between experiment and modelling was less than 10%, which confirms the validity of the model used.

The experimental results show that at low reverse current densities the structure returns to the system up to 90% of the energy lost during switching, the share of the active component is small (experiment N^o 2). At maximum operating voltage on the structure and increasing reverse current density (experiments N^o 1 and 3), the specific value of reactive losses remains unchanged, while the value of active losses increases. At the same time, the high switching speed of dU/dt is achieved at higher reverse current densities.

Figure 2 shows the oscillograms of current, voltage, power, and energy loss for the N^o 1 experiment (experimental data are represented by solid lines and simulation results — dashed lines). As can be seen from the figure, at the stage of direct current flow a small part of energy is dissipated on the structure, the voltage on the structure is small. At polarity reversal the diode conduction mode is preserved for some time, the reverse current value increases, the voltage

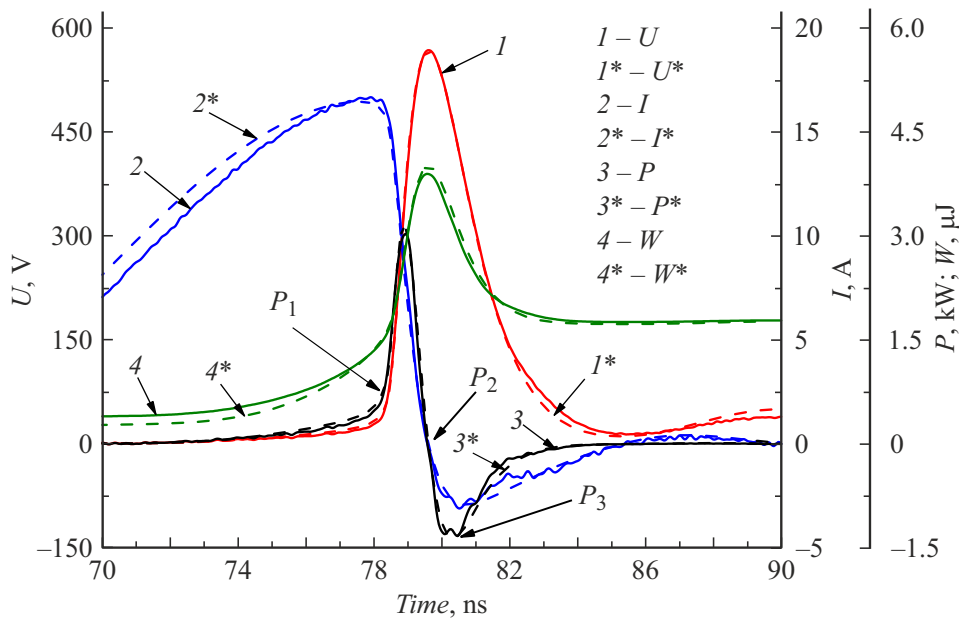


Figure 2. Oscillograms of current, voltage, power and energy loss for the № 1 experiment. Experimental data are represented by solid lines and modelling results — dashed lines.

on the structure also increases (slow section of voltage growth up to the moment marked by the point P_1 in Fig. 2).

Up to the moment P_1 , minority charge carriers are carried away from the DSRD base, electron-hole plasma fronts are formed, which move towards each other under the action of the electric field (Fig. 3, a). The energy losses at this stage are active and lead to the warming up of the structure. This is followed by a rapid current cut-off stage. At the P_1 time instant, the plasma fronts meet near the p - n -junction, further the reverse current flow is possible only due to the current of equilibrium carriers, which leads to the formation of the bulk charge region near p - n -junction (Fig. 3, a). The figure shows that in the investigated structure the end of the process of extraction of nonequilibrium plasma occurs not in the plane of p - n -junction, which slows down the switching process of the structure, because the removal of holes from the p -region begins before the end of extraction of non-equilibrium carriers in the n -base. In addition, the n^+ -substrate shows accumulation of minority holes due to two factors: its weak doping ($N_D = 3 \cdot 10^{18} \text{ cm}^{-3}$) and the blurred boundary between the n -base and the n^+ -substrate. The accumulation of holes in the n^+ -region in turn leads to a decrease in the injection efficiency. It is possible to optimize the structure to obtain the best transition characteristics by varying the thicknesses of the low-alloyed regions and transferring the p - n -junction to the point where the modulated depletion waves should converge when the nonequilibrium plasma is ejected from the base of the structure. The thicknesses of the low-alloyed regions should approximate the condition $w_n/w_p \sim \mu_p/\mu_n$, where

w_n and w_p — the thicknesses of the low-alloyed n - and p - regions, μ_p and μ_n — the hole and electron mobilities, respectively.

The electric field strength reaches a maximum and propagates to the boundaries of p^+ - and n^+ -regions (Fig. 3, b) by the moment of time marked by the point P_2 in Fig. 2. Losses at this stage are reactive and will be returned to the system. From the P_2 time instant, the stored energy is returned due to the discharge of the barrier capacitance p - n -junction (Fig. 3, c).

The energy loss dependence of the reverse current density when switching the p^+ - p - n - n^+ -structure from the conducting state to the blocking state has been investigated in work. The reactive component of energy loss — the energy stored as a charge in the barrier capacitance p - n -junction and then fed back into the system is considered. It is shown that as the reverse current density increases, the share of the active component of energy losses increases, which leads to the heating of the structure, which imposes a limitation on the maximum repetition rate, causes instability of pulse amplitude and shape, as well as thermal drift of the delay in the formation of the output pulse relative to the trigger pulse. At the same time, a high reverse current density is required to maximise the switching speed of the dU/dt structure. Thus, there is no universal mode of operation of DSRD, which provides the best switching characteristics in conjunction with the lowest energy losses. The mode of operation should be selected based on the objectives: greatest system efficiency or fastest performance.

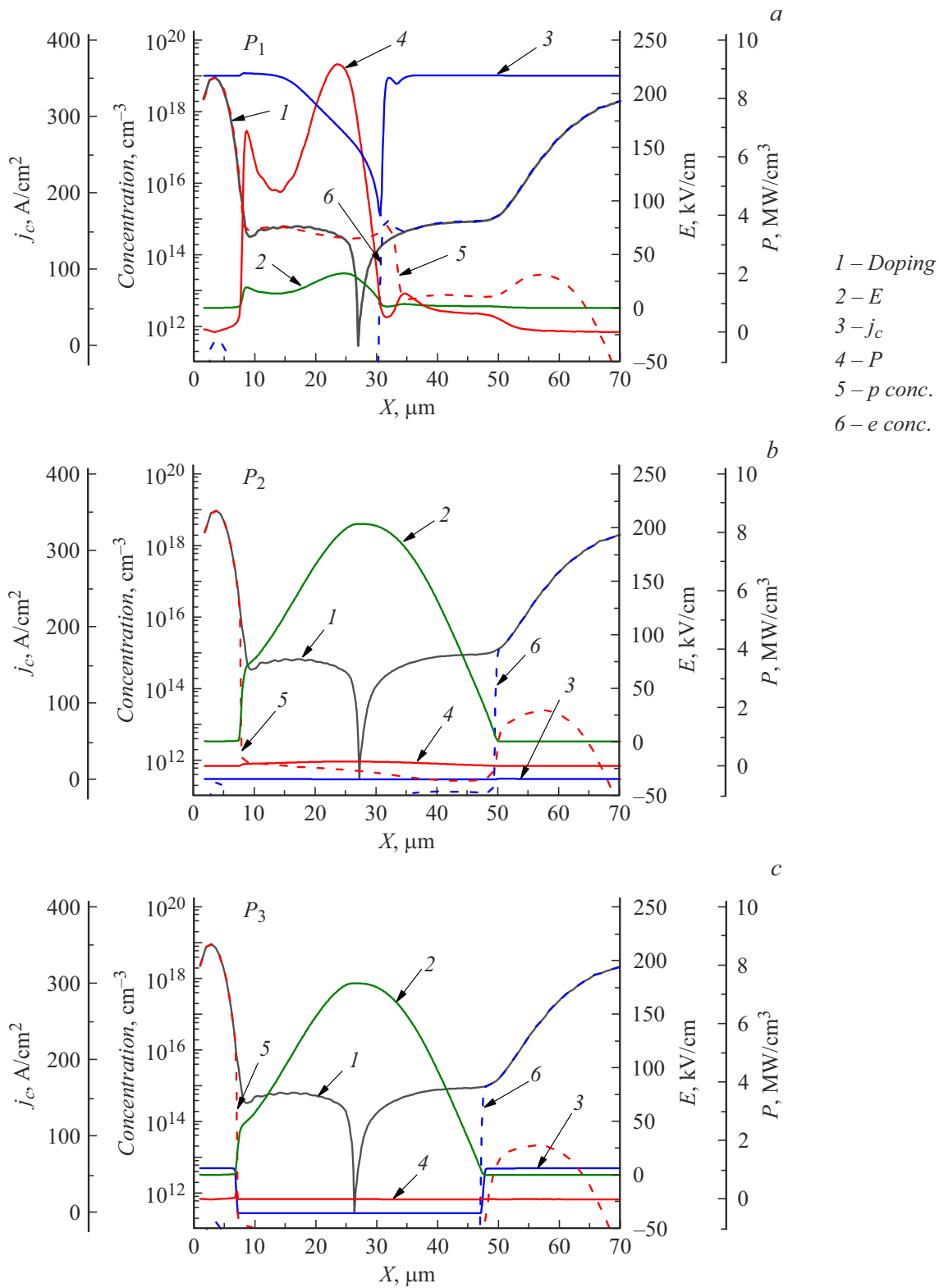


Figure 3. Distribution of dopant concentration (*Doping*), electrons (*e conc.*), holes (*p conc.*), electric field strength (E), conduction current (j_c), and emitted power (P) for the time points P_1 (a), P_2 (b), and P_3 (c).

Funding

This work was supported by the Ministry of Science and Education of the Russian Federation (project № 075-15-2020-790).

Conflict of interest

The authors declare that they have no conflict of interest.

References

- [1] A.F. Kardo-Sysoev, in *Ultra-wideband radar technology*, ed. by J.D. Taylor (CRC Press, Boca Raton–London–N.Y.–Washington, 2001), p. 214–299.
- [2] I.V. Grekhov, V.M. Efanov, A.F. Kardo-Sysoev, S.V. Shenderoy, *Solid-State Electron.*, **28** (6), 597 (1985). DOI: 10.1016/0038-1101(85)90130-3
- [3] V.A. Ilyin, A.V. Afanasyev, Yu.S. Demin, B.V. Ivanov, A.F. Kardo-Sysoev, V.V. Luchinin, S.A. Reshanov, A. Schöner, K.A. Sergushichev, A.A. Smirnov, *Mater. Sci. Forum*, **924**, 841 (2018). DOI: 10.4028/www.scientific.net/MSF.924.841
- [4] I.V. Grekhov, G.A. Mesyats, *Phys. Usp.*, **48** (7), 703 (2005). DOI: 10.1070/pu2005v048n07abeh002471.
- [5] X. Yang, Y. Li, H. Wang, Z. Li, Z. Ding, *J. Appl. Phys.*, **109** (1), 014917 (2011). DOI: 10.1063/1.3531624
- [6] A.G. Lyublinsky, S.V. Korotkov, Y.V. Aristov, D.A. Korotkov, *IEEE Trans. Plasma Sci.*, **41** (10), 2625 (2013). DOI: 10.1109/TPS.2013.2264328
- [7] Y. Sharabani, I. Shafir, S. Zoran, A. Raizman, A. Sher, Y. Rosenwaks, D. Eger, *IEEE Electron Dev. Lett.*, **37** (8), 1041 (2016). DOI: 10.1109/LED.2016.2584541
- [8] A.G. Lyublinsky, A.F. Kardo-Sysoev, M.N. Cherenev, M.I. Vexler, *IEEE Trans. Power Electron.*, **37** (6), 6271 (2022). DOI: 10.1109/TPEL.2021.3139536
- [9] D.M. Caughey, R.E. Thomas, *Proc. IEEE*, **55** (12), 2192 (1967). DOI: 10.1109/PROC.1967.6123
- [10] J. Dorkel, Ph. Leturcq, *Solid-State Electron.*, **24** (9), 821 (1981). DOI: 10.1016/0038-1101(81)90097-6
- [11] D.J. Roulston, N.D. Arora, S.G. Chamberlain, *IEEE Trans. Electron Dev.*, **29** (2), 284 (1982). DOI: 10.1109/T-ED.1982.20697
- [12] M.E. Law, E. Solley, M. Liang, D.E. Burk, *IEEE Electron Dev. Lett.*, **12** (8), 401 (1991). DOI: 10.1109/55.119145
- [13] J.G. Fossum, D.S. Lee, *Solid-State Electron.*, **25** (8), 741 (1982). DOI: 10.1016/0038-1101(82)90203-9

Translated by 123